

High-Energy Metal to Ligand Charge-Transfer States in Ruthenium-Diimine Complexes

Michael L. Myrick and M. Keith De Armond*

Chemistry Department, New Mexico State University, Las Cruces, New Mexico 88003
(Received: February 27, 1989)

Earlier emission and absorption contours for the $[\text{Ru}(\text{bpy})_2(\text{dppe})]^{2+}$ complex were anomalous. In addition, the photoselection spectra (emission and excitation) differ from that found previously for $(\text{bpy})_2$ complexes. Speculation was that these differences result from the high-energy metal to ligand charge-transfer (MLCT) state in this complex. Consequently, a number of bis Ru(II) chelate complexes with varying energy MLCT states were examined to rationalize these experimental results. The results with use of perturbation theory demonstrate an interaction between the singlet MLCT states and the $\pi-\pi^*$ states for these materials. The correlations of the emission Stokes shift and the zero-order energy of the singlet MLCT state indicate that singlet absorption and triplet emission derive from states of different orbital configuration. Predictions of the symmetry of the absorbing singlet and emitting triplet from a simple model are consistent with the results obtained earlier from the interchromophoric coupling model.

Introduction

In the course of studies reported earlier,¹ a complex, $[\text{Ru}(\text{bpy})_2(\text{dppe})](\text{PF}_6)_2$, was found that possessed relatively high-energy metal to ligand charge-transfer (MLCT) absorbance and ³MLCT emission bands. Structure in the absorption spectrum of this complex was different from that seen for other complexes with Ru-bpy absorbance. Also, the emission was different from the normal Ru-diimine luminescence, with a more pronounced low-energy shoulder relative to its high-energy maximum. In addition, the photoselection across the ¹MLCT absorption did not attain values typical of bis chelates, reaching $P = 0.22$ rather than $P \approx 0.33-0.35$. Structure in the SSEXp was noticeably absent across the ¹MLCT absorbance. The decay time of the luminescence at 77 K was substantially longer than is typically observed for the Ru-bpy unit, implying that the luminescent state was altered in some manner. This is consistent with the observation that luminescence for the complex only occurred in frozen solution, with fluid solutions nonemissive.

These observations on the nature of a complex with high-energy MLCT states led to the work presented here, in which a variety of molecules with varying MLCT energies were systematically examined. Some of the complexes presented here exhibit luminescence at very high energy, glowing blue upon excitation rather than the typical orange-red. Indeed, some of the materials have MLCT states at energies so high that the $\pi-\pi^*$ states of the ligands are lower in energy, producing long-lived excited states similar to that of $[\text{Rh}(\text{bpy})_3]^{3+,2,3}$

The principal motivation for these studies is to clarify the interactions occurring in high-energy MLCT states that produce the data exhibited by such complexes.

Experimental Section

$[\text{Ru}(\text{bpy})_2(\text{dppe})](\text{PF}_6)_2$ (dppe = 1,2-bis(diphenylphosphino)ethane) was prepared⁴ by refluxing 0.1 g of $[\text{Ru}(\text{bpy})_2\text{Cl}_2] \cdot 3\text{H}_2\text{O}$ with 0.4 g of dppe ligand in 60 mL of 1:1 $\text{H}_2\text{O}/\text{EtOH}$. The reaction was kept under $\text{N}_2(\text{g})$ for the duration. After a 6-h reflux, the reaction mixture was deep red, indicating that little reaction had occurred. A large amount of the dppe ligand appeared to be undissolved at this time. Reflux was continued for 2 weeks, at the end of which the solution was yellow with an orange tinge. The reaction mixture was filtered to remove unreacted ligand, and KPF_6 was added to form a yellow precipitate. This precipitate was filtered from the hot solution, and the filtrate was cooled to room temperature. At this time, more yellow

precipitate formed in the filtrate and was collected. The initial collection from the hot yellow-brown solution was $[\text{Ru}(\text{bpy})_2(\text{dppe})](\text{PF}_6)_2$ with some unknown impurity, likely $[\text{Ru}(\text{bpy})_2(\text{dppe})\text{Cl}](\text{PF}_6)$. However, the second collection, though of much less total weight, was bright yellow and was pure as the emission spectrum was invariant to different excitation energies.

$[\text{Ru}(\text{bpy})_2(\text{dppe})](\text{PF}_6)_2$ was synthesized by a variation of the above technique. The procedure of Krause⁵ was used to synthesize $[\text{Ru}(\text{bpy})_2\text{Cl}_2]$. Stirring was begun with 0.042 g of this material in 50 mL of H_2O . This was purged with $\text{N}_2(\text{g})$ for 15 min, and 0.400 g of dppe ligand was added and reflux was begun. The use of H_2O solvent alone helped to dissolve the dppe, though some ligand was still undissolved. Initially, the mixture was an opaque yellow-green that upon reflux became dark green. After 6 days, the solution had become yellow-orange and slowly became more yellow until, after 2 weeks, the reaction was stopped. The reaction mixture was filtered and $\text{KPF}_6(\text{aq})$ was added. The resulting yellow-brown precipitate was collected after the suspension was allowed to cool to room temperature. Purification of the complex was accomplished by column chromatography on Sephadex LH-20 in ethanol. The band began to move immediately, and no separation was apparent to the naked eye; rather, the band appeared to spread and disperse. However, collections taken at the band head were pure. Those taken near the tail contained significant impurities.

$[\text{Ru}(\text{bpy})_2(\text{dmpe})](\text{PF}_6)_2$ (dmpe = 1,2-bis(dimethylphosphino)ethane) was prepared by refluxing 0.1 g of $[\text{Ru}(\text{bpy})_2\text{Cl}_2]$ with 0.2 mL of the liquid dmpe ligand in 60 mL of 1:1 $\text{EtOH}/\text{H}_2\text{O}$ under $\text{N}_2(\text{g})$. The reaction mixture was allowed to reflux for $3\frac{1}{2}$ days, though the reaction appeared to be over after 10 h. The reaction mixture was yellow-orange, and the addition of $\text{KPF}_6(\text{aq})$ gave no precipitate. Partial evaporation with a rotary evaporator yielded a large amount of yellow-orange precipitate. This was collected by filtration and passed through a Sephadex LH-20 column in acetone, resulting in a large yellow band with large R_f followed by a smaller band. Fractions were collected of the large band. The first fraction was found to be impure, while later fractions were pure.

$[\text{Ru}(\text{bpy})_2(\text{CNMe})(\text{CN})]^+$ and $[\text{Ru}(\text{bpy})_2(\text{CNMe})_2]^{2+}$ (CNMe = methyl isocyanide) were provided by Scandola.⁶ $[\text{Ru}(\text{i-biq})_3](\text{PF}_6)_2$ (i-biq = 2,2'-biisoquinoline) and i-biq ligand were provided by Belser and Von Zelewsky. $[\text{Ru}(\text{bpy})_2(\text{en})](\text{ClO}_4)_2$ was available from previous studies.

$[\text{Ru}(\text{bpy})_2(\text{CNH})_2](\text{SO}_4)$ was prepared by dissolving $[\text{Ru}(\text{bpy})_2(\text{CN})_2]$ in sulfuric acid. Studies of this complex were performed in this glass only. $[\text{Ru}(\text{bpy})_2(\text{CNMe})(\text{CNH})]^{2+}$ was

(1) Myrick, M. L.; Blakley, R. L.; De Armond, M. K. *J. Phys. Chem.*, in press.

(2) Halper, W.; De Armond, M. K. *Chem. Phys. Lett.* 1974, 24(1), 114.
(3) (a) Tinti, D.; El-Sayed, M. *J. Chem. Phys.* 1971, 54(6), 2529. (b) El-Sayed, M. *Accts. Chem. Res.* 1971, 4, 23. (c) Hall, L.; Owens, D.; El-Sayed, M. *Mol. Phys.* 1971, 20(6), 1025. (d) Hall, L.; El-Sayed, M. *Chem. Phys.* 1975, 8, 272.

(4) Rillema, D.; Allen, G.; Meyer, T.; Conrad, D. *Inorg. Chem.* 1983, 22, 1617.

(5) Krause, R. *Inorg. Chim. Acta* 1977, 22, 209.

(6) (a) Indelli, M.; Bignozzi, C.; Marconi, A.; Scandola, F. In *Photochemistry and Photophysics of Coordination Compounds*; Yersin, H., Vogler, A., Eds.; Springer-Verlag: Berlin, 1987; p 159. (b) Private communication with the author. (c) Indelli, M.; Bignozzi, C.; Marconi, A.; Scandola, F. *J. Am. Chem. Soc.* 1988, 110, 7381.

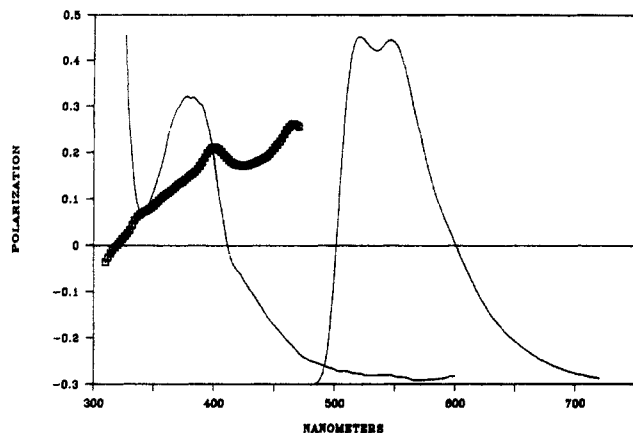


Figure 1. Absorption, emission, and steady-state photoselection of the $[\text{Ru}(\text{bpy})_2(\text{dppe})](\text{PF}_6)_2$ complex [dppe = 1,2-bis(diphenylphosphino)ethane] in ethanol at 77 K. Emission is uncorrected for detector response. Absorption is base-line corrected but uncorrected for contraction of solvent.

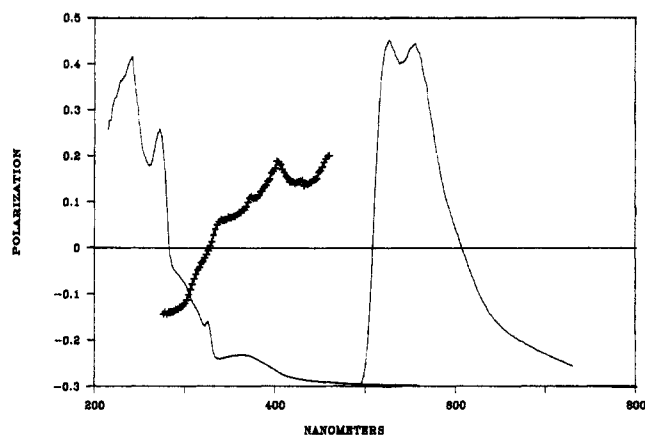


Figure 2. Absorption, emission, and steady-state photoselection of the $[\text{Ru}(\text{bpy})(\text{dppe})_2](\text{PF}_6)_2$ complex in ethanol at 77 K.

prepared in an analogous fashion.

Photoselection was performed on an instrument previously described, now interfaced to a Zenith Model Z-158 computer. Most studies were performed in EtOH solvent.

Lifetime measurements were performed with excitation from the 337-nm line of a N_2 laser. Luminescence was detected with a $3/4\text{-m}$ Czerny-Turner monochromator and a Hamamatsu Model R-955 photomultiplier tube. Time resolution was provided by a Stanford Research Systems Model SR 250 boxcar averager interfaced to a Zenith Model Z-158 computer.

Steady-state luminescence measurements were made with the same instrument used for photoselection, by removing the rotating polarizer. Emission spectra were uncorrected for detector response. All spectra reported were taken at 77 K.

Room-temperature and 77 K electronic absorption spectra were recorded with a Cary Model 14 absorption spectrometer interfaced to a Zenith Model Z-100 computer with programming by On-Line Instrument Systems. Room-temperature spectra were recorded in quartz cuvettes for the near-UV. Low-temperature spectra were recorded in polystyrene cuvettes in an Oxford Instruments $\text{N}_2(\text{L})$ optical cell modified for the Cary 14. Polystyrene cells were necessary for these measurements as the contraction and expansion of the solvent during freezing generally shattered the quartz cuvettes. All absorption measurements are corrected for base-line errors

Results

Table I summarizes the maxima of the absorbance, emission, and photoselection for the complexes, as well as lifetimes where available. Data for $[\text{Ru}(\text{bpy})_3]^{2+}$ and $[\text{Rh}(\text{bpy})_3]^{3+}$ are included as a reference.⁷

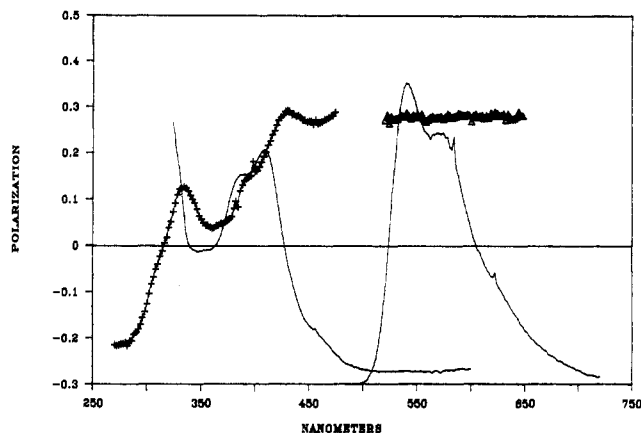


Figure 3. Absorption, emission, and steady-state photoselection of the $[\text{Ru}(\text{bpy})_2(\text{CNMe})(\text{CN})]^+$ complex (CNMe = methyl isocyanide) in ethanol at 77 K.

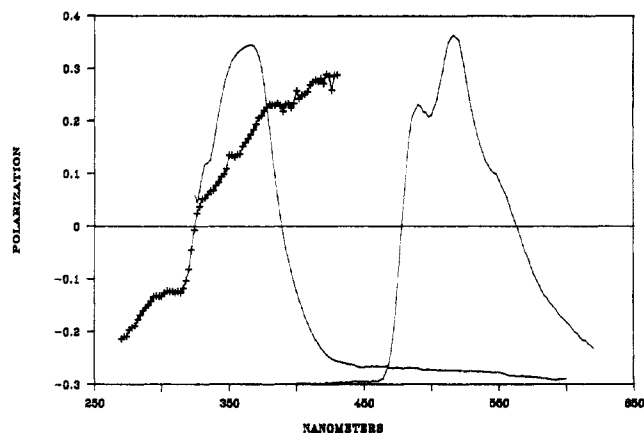


Figure 4. Absorption, emission, and steady-state photoselection of the $[\text{Ru}(\text{bpy})_2(\text{CNMe})_2]^{2+}$ complex in ethanol at 77 K.

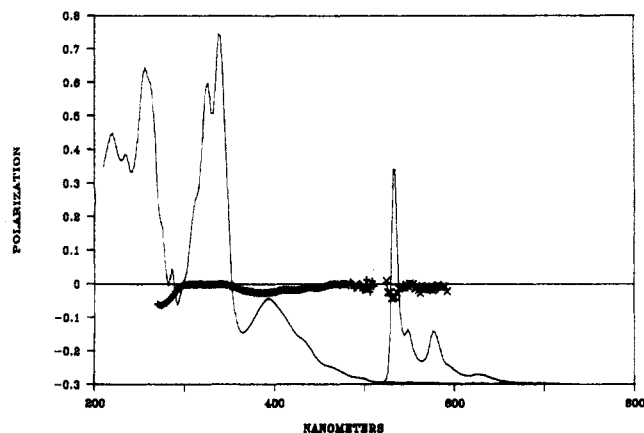


Figure 5. Absorption, emission, and steady-state photoselection of the $[\text{Ru}(\text{i-biq})_3](\text{PF}_6)_2$ complex (i-biq = 2,2'-biisoquinoline) in ethanol at 77 K.

Absorption, steady-state excitation polarization (SSEXP), and luminescence for $[\text{Ru}(\text{bpy})_2(\text{dppe})](\text{PF}_6)_2$ in ethanol are given in Figure 1. The same data are presented in Figure 2 for $[\text{Ru}(\text{bpy})(\text{dppe})_2](\text{PF}_6)_2$. Data for $[\text{Ru}(\text{bpy})_2(\text{CNMe})(\text{CN})]^+$, $[\text{Ru}(\text{bpy})_2(\text{CNMe})_2]^{2+}$, and $[\text{Ru}(\text{i-biq})_3](\text{PF}_6)_2$ are shown in Figures 3–5, respectively. The protonated forms of the cyanide complexes were produced by dissolution in $\text{H}_2\text{SO}_4/\text{H}_2\text{O}$ (1:1), and data for $[\text{Ru}(\text{bpy})_2(\text{CNMe})(\text{CNH})]^{2+}$ is shown in Figure 6.

Absorption. In the complexes under study in this chapter, MLCT states at high energy are considered. For all but $[\text{Ru}$

TABLE I: Data for Complexes with High-Energy MLCT States

complex	emiss max	abs max		P_{extreme}^a	$\tau/\mu\text{s}$
		MLCT	$\pi-\pi^*$		
[Ru(bpy) ₂ (dppe)](PF ₆) ₂	515 (19.4)	380 (26.3)	277 (36.1)	0.21 (400)	20.0
[Ru(bpy)(dppe) ₂](PF ₆) ₂	523 (19.1)	361 (27.7)	272 (36.8)	0.19 (402)	18.2
[Ru(bpy) ₂ (dmpe)](PF ₆) ₂	556 (18.0)	415 (24.1)	280 (35.7)	0.28 (430)	
[Ru(bpy) ₂ (CNMe)(CN)] ⁺	542 (18.5)	408 (24.5)	281 (35.6)	0.29 (430)	
[Ru(bpy) ₂ (CNMe) ₂] ²⁺	490 (20.4)	366 (27.3)	269 (37.2)	0.23 (380)	
[Ru(i-biq) ₃](PF ₆) ₂	534 (18.2)	394 (25.4)	338 (29.6)	-0.03 (386)	
[Ru(bpy) ₂ (en)](ClO ₄) ₂ ^b	670 (14.9)	352 (28.4)	287 (34.8)	0.18 (380)	1.1
[Ru(bpy) ₂ (CNH) ₂] ²⁺	512 (19.5)	352 (28.4)	261 (38.3)	0.17 (370)	
	478 (20.8) ^c				
[Ru(bpy) ₂ (CNMe)(CNH)] ²⁺	510 (19.6)	354 (28.2)	263 (38.0)	0.18 (384)	
	480 (20.8) ^c				
[Ru(bpy) ₃] ²⁺	578 (17.3)	460 (21.7)	285 (35.1)	0.23 (468)	
[Rh(bpy) ₃] ³⁺ ^d	450 (22.2) ^d		239 (41.8) ^d		

^a Usually P_{max} , but for [Ru(i-biq)₃]²⁺ is P_{min} . ^b Absorbing MLCT state studied is $D\pi(\chi)$. ^c Estimated maximum of first band in emission. ^d Reproduced from ref 7.

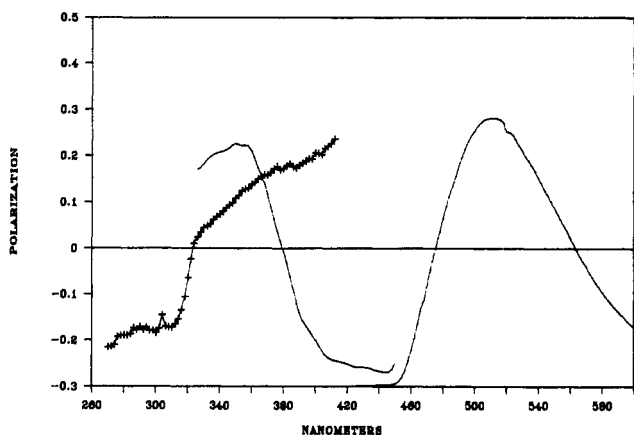


Figure 6. Absorption, emission, and steady-state photoselection of the [Ru(bpy)₂(CNMe)(CNH)]²⁺ complex in 1:1 H₂SO₄/H₂O at 77 K.

(bpy)₂(en)](ClO₄)₂, these states derive from the $d-\pi^*(\psi)$ (Orgel⁸ notation) transition, involving the lowest energy π^* orbital of bipyridine. For the latter complex, the transition under discussion derives from $d-\pi^*(\chi)$ parentage, involving the promotion of a metal electron to the second unoccupied π^* molecular orbital of bipyridine, since this transition occurs at approximately the same energy as the lowest ¹MLCT of the other complexes.

From study of the absorption spectra shown in Figures 1–5, it is clear that the energy of the pertinent ¹MLCT transition varies widely among these complexes. The complexes of bipyridine have ¹MLCT absorbances that have maxima between 360 ($27.8 \times 10^3 \text{ cm}^{-1}$) and 415 nm ($24.1 \times 10^3 \text{ cm}^{-1}$). Also, the band shapes of these absorbances vary. Those that occur toward lower energy possess dual maxima in the charge-transfer region. This has been shown previously to be due to vibronic transitions coupling, principally, to a single electronic transition.¹ The ¹MLCT bands that appear at higher energy are skewed to high energy, perhaps indicating increasing distortion and charge-transfer character in the absorbance. Note also that a rough correlation between the energy of the ¹MLCT absorbance and the $\pi-\pi^*$ absorbance of the ligand occurs (Figure 7). Apparently, for molecules with low-lying ¹MLCT states, the $\pi-\pi^*$ transition maximizes at approximately 287 nm ($35.7 \times 10^3 \text{ cm}^{-1}$). As the energy of the ¹MLCT state increases beyond approximately $25 \times 10^3 \text{ cm}^{-1}$ (400 nm), some perturbation of the $\pi-\pi^*$ levels begins to occur, elevating the energy of one or more states. Note also that as the $\pi-\pi^*$ state is raised in energy, bands that had previously been lost beneath that intense transition are revealed. This is illustrated in Figures 1, 2, 4, and 6.

Emission. The variation of the luminescence of these molecules is also large, with maxima occurring between 490 ($20.4 \times 10^3 \text{ cm}^{-1}$) and 556 nm ($18.0 \times 10^3 \text{ cm}^{-1}$). Those molecules that exhibit

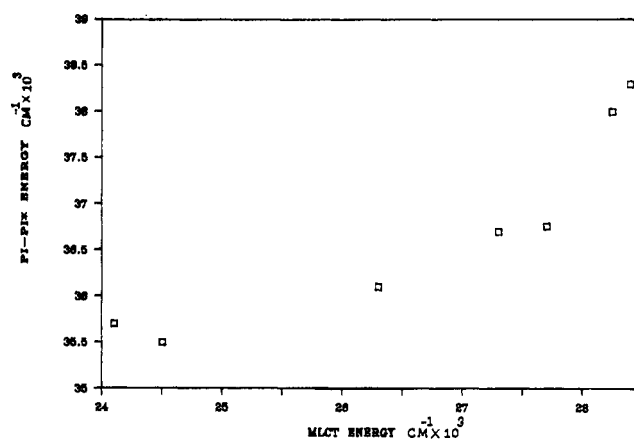


Figure 7. $E(\pi-\pi^*)$ vs $E(\text{MLCT})$, variation of the energy of the ¹ $\pi-\pi^*$ absorbance of each of the complexes as a function of the energy of the maximum of the ¹MLCT transition. Each of these studies was performed in ethanol. Energies of the ¹ $\pi-\pi^*$ state were obtained from room-temperature measurements, while those of the ¹MLCT state were obtained from frozen solution.

higher energy phosphorescences also exhibit a spectrum skewed to low energy, possibly also indicative of greater distortion in the excited state. Indeed, the luminescence spectra of [Ru(bpy)₂(CNH)₂]²⁺ and [Ru(bpy)₂(CNMe)(CNH)]²⁺ (Figure 6) appear to have high-energy shoulders near 480 nm ($20.1 \times 10^3 \text{ cm}^{-1}$) that are obscured by much larger bands at lower energy. Thus, these spectra seem to be poorly resolved and broad. Interestingly, these emission energies are approaching the energies at which the ³ $\pi-\pi^*$ state (450 nm) is expected to appear as seen, for example, in [Rh(bpy)₃]³⁺² and [Ru(bpy)(CNMe)₂]²⁺.⁶

The decay times that have been determined for some of the complexes presented here are significantly longer than those of most other molecules with Ru-bpy emitting chromophores. The luminescence found for many Ru-bpy luminophores, occurring at or near 580 nm ($17.2 \times 10^3 \text{ cm}^{-1}$), is found to be approximately 4–6 μs at 77 K. The 20- μs decay of [Ru(bpy)₂(dppe)]²⁺ is significantly longer, though still presumably of ³MLCT origin. The still longer decay of [Ru(i-biq)₃]²⁺ results from a distinct change in the nature of the emitting state, from ³MLCT to ³ $\pi-\pi^*$, and the lifetime that was originally determined by Balzani and Von Zelewsky⁹ is consistent with the results obtained for the rhodium species.²

Photoselection. Another notable feature of the excited states in this series of complexes is that the photoselection (P) that is determined across the ¹MLCT absorption bands is different from that found for most species.¹ Perhaps most surprising is that the photoselection spectrum of [Ru(bpy)(dppe)₂]²⁺, which should be

relatively featureless and give large polarizations by analogy with other monochelated Ru–diimine complexes, actually exhibits structure across the singlet transition and has a small P . Curiously, the analogous bis(diimine) complex, $[\text{Ru}(\text{bpy})_2(\text{dpe})]^{2+}$, appears to show much the same type of SSEXP profile as this monomeric complex, despite the presumed presence of variant polarizations within the $^1\text{MLCT}$ absorbance of this species with two chromophores.

Discussion

The phenomena presented above indicate the presence of energy and wave function perturbations to the MLCT manifold in these complexes. The curvature of the plot in Figure 7, giving the variation of $\pi\text{--}\pi^*$ absorption with $d\text{--}\pi^*$ absorption, indicates that these transitions may be coupled in some fashion, with the coupling increasing in magnitude as the $^1\text{MLCT}$ manifold moves toward higher energy. Qualitatively, the ICC model¹⁰ supplies a rationalization of the polarization properties of most Ru–diimine chelates, but some deviations do occur. In particular, the photoselection of $[\text{Ru}(\text{bpy})_2(\text{dpe})]^{2+}$ indicates that the structure for that complex was unusual, and the maximum value of P obtained on the red edge of the $^1\text{MLCT}$ absorbance was significantly lower than the "normal" behavior seen for most bis chelates in the cis configuration. The behavior seen for $[\text{Ru}(\text{bpy})_2(\text{en})]^{2+}$ and $[\text{Ru}(\text{biq})_3]^{2+}$, both of which produce higher values than typically obtained, may seem to suggest that no "quantized" (e.g., 0.23 for tris complexes, 0.33 for bis) values of P actually occur but rather a regular dependence of P_{max} upon the energy of absorption and emission for the complexes is occurring. A simplistic view of this might be that complexes produce larger values of P when their MLCT states are at relatively lower energy; quantization of P occurs because most complexes have emission near the same energy.

The effort in this discussion, then, is to demonstrate that the low values obtained for the phosphine-substituted complex and other complexes with high-energy MLCT states are due to phenomena that do not occur in most species with lower lying states. Hence, the values obtained for the species presented earlier are indeed due to processes distinct from those occurring in the unusual complexes presented here.

Absorbing States. It is generally assumed, in the treatment of wave functions produced by the interaction of a transition metal and a π -chelate ligand, that the wave functions produced may be described as metal-localized and ligand-localized. Still, some mixing of wave functions of metal ion and ligands is indicated by numerous results in the literature. For instance, the reduced C=O stretching frequency in metal carbonyl complexes is attributable to the back-donation of electron density from the metal center to a π^* orbital of the ligand that is of the proper symmetry to combine with the t_{2g} orbital set of the metal. Also, the relative position of some ligands in the spectrochemical series is due in part to π back-bonding. Ligands such as CN^- , CNMe , and bpy all produce larger ligand field splitting of metal d orbitals than similar nonaromatic ligands, such as ethylenediamine. As the series of complexes under study here illustrate, phosphine ligands, particularly those with aromatic substituents, increase ligand field splitting of ruthenium compared to bpy ; this is attributable to vacant d orbitals on the phosphorus atom that again accept electron density from the metal. An additional example of the mixing of metal and ligand wave functions is available from charge-transfer absorption. As shown by Day and Sanders,¹¹ most of the intensity that is obtained by such transitions results from such mixing.

The energy of the $\pi\text{--}\pi^*$ transition should at first glance be relatively independent of the magnitude of ligand field stabilization of the metal since any overall charge on the ligand developed by electron donation to the d_{π^*} orbitals of the metal by the nonbonding

electrons of the nitrogen atoms in the chelate serves to lower the energy of the π^* orbital of the ligand but also lowers the energy of the π orbital, resulting in a negligible effect upon the $\pi\text{--}\pi^*$ transition.

However, since an interaction between the metal d_{π^*} orbitals and the ligand π^* orbital serves to raise the energy of the latter, then the effect of stronger field ligands such as CNMe would be to lower the energy of the $\pi \rightarrow \pi^*$ transition slightly. This is due to the increased zero-order energy separation between π^* and d_{π^*} orbitals of the metal and the consequent reduction in interaction between the state wave functions. But the $\pi \rightarrow \pi^*$ transition is observed to increase in energy as the $^1\text{MLCT}$ transition increases in energy; thus, this metal–ligand orbital interaction cannot be the source of the trend in the $\pi \rightarrow \pi^*$ transitions.

A possibility remains that direct interactions between the $\pi\text{--}\pi^*$ state and the $d\text{--}\pi^*$ state occur. Qualitatively, any such coupling, should force the ligand-centered transition higher in energy as the perturbing $d\text{--}\pi^*$ state approaches the $\pi\text{--}\pi^*$ state.

To focus quantitatively on the interactions of the high-energy states of these complexes, examination will be restricted to the two transitions for which relative energies and polarizations are most easily obtainable, the $d\text{--}\pi^*$ and $\pi\text{--}\pi^*$ singlet absorbances. Energies and polarizations of the $d\text{--}\pi^*$ states are easily determined from absorption and SSEXP spectra of the complexes, since the visible region of absorbance is dominated by these charge-transfer transitions. The $\pi\text{--}\pi^*$ transition is not so well separated from others in the UV region but is generally apparent due to the large oscillator strength of the absorbance, which causes it to dominate other transitions in that region.

Certainly, for bipyridine, the $d\text{--}\pi^*(\chi)$ transition appears in the UV region for most complexes with ruthenium and is frequently difficult to separate from the $\pi\text{--}\pi^*$ band. Indeed, in all the complexes (with the exception of $[\text{Ru}(\text{bpy})_2(\text{en})]^{2+}$), this absorbance is strongly overlapped with the $\pi\text{--}\pi^*$ band. To treat the interaction between the $d\text{--}\pi^*(\psi)$ transition and the $\pi\text{--}\pi^*$ absorbance with perturbation theory by focusing only on these two states, we must neglect any interaction with the $d\text{--}\pi^*(\chi)$ state. We may presume that interactions between the latter state and the $\pi\text{--}\pi^*$ are weak for some reason (e.g., the lack of any effective perturbation operator), or we must assume that this state and the $\pi\text{--}\pi^*$ interact in all the complexes under study with nearly the same magnitude. If either of these conditions are obtained, we may successfully neglect contributions from the higher MLCT state while retaining some measure of accuracy in our calculations.

To analyze the variation of the energy of absorbance of the $\pi\text{--}\pi^*$ state with the separation of $^1\pi\text{--}\pi^*$ and $^1\text{MLCT}$ states, we turn to simple perturbation theory (PT). The simplest form of PT that will encompass the phenomena analyzed is second-order energy perturbation theory. The equation that governs the treatment is given as eq 1, where E^2 is the second-order correction

$$E^2 = \frac{\langle \psi_1 | \hat{O} | \psi_2 \rangle \langle \psi_2 | \hat{O} | \psi_1 \rangle}{E_1^0 - E_2^0} \quad (1)$$

to the energy of a state, E_1^0 is the zero-order energy of state 1, E_2^0 is the zero-order energy of state 2, and \hat{O} is a general perturbation operator.

As expected, this simple formula demonstrates that when two states interact, they mix and separate in energy. To the order of approximation given here, the increase of energy of the state that is higher lying exactly equals that of the stabilization of the lower lying state. This approximation fails when higher orders of PT are utilized but suffices for the present investigation.

To make use of the above equation, zero-order energies for the states involved must be estimated. For the $\pi\text{--}\pi^*$ state, this energy is relatively simple to approximate. Simply choose some complex with bipyridine chelated to ruthenium that has a $^1\text{MLCT}$ absorbance that is as far red-shifted as possible. This is necessary since the free ligand has a different geometry from coordinated bipyridine, and we wish to include as much of the effect resulting from the overlap of the π^* with the ruthenium t_{2g} set as possible. For this purpose, we choose $[\text{Ru}(\text{bpy})_2(\text{CO}_3)] \cdot 2\text{H}_2\text{O}$, originally prepared as an intermediate in the synthesis of *trans*-[Ru-

(10) Myrick, M.; Blakley, R.; De Armond, M. K.; Arther, M. L. *J. Am. Chem. Soc.* **1988**, *110*, 1325.

(11) (a) Day, P.; Sanders, N. *J. Chem. Soc. A* **1967**, 1530. (b) Day, P.; Sanders, N. *J. Chem. Soc. A* **1967**, 1536.

TABLE II: Perturbation Energy, Difference between Approximate Zero-Order $\pi-\pi^*$ and MLCT States, and Stokes Shift for Complexes with High-Energy MLCT States

complex	$E_{\pi-\pi^*} - 34.8 \times 10^3 \text{ cm}^{-1}$ ^{a,c}	E_{MLCT}^0 ^{a,d}	E_{MLCT}^0 ^e	Stokes shift ^{a,e}
[Ru(bpy) ₂ (dppe)] ²⁺	1.3	27.6	0.139	6.9
[Ru(bpy)(dppe) ₂] ²⁺	2.0	29.7	0.196	8.6
[Ru(bpy) ₂ (dmpe)] ²⁺	0.9	25.0	0.102	6.1
[Ru(bpy) ₂ (CNMe)(CN)] ⁺	0.8	25.3	0.105	6.0
[Ru(bpy) ₂ (CNMe) ₂] ²⁺	2.4	29.7	0.196	6.9
[Ru(bpy) ₂ (CNH) ₂] ²⁺	3.5	31.9	0.345	7.6 ^f
[Ru(bpy) ₂ (CNMe)(CNH)] ²⁺	3.2	31.4	0.294	7.4 ^f

^a Units of 10^3 cm^{-1} . ^b Units of $(10^3 \text{ cm}^{-1})^{-1}$. ^c $34.8 \times 10^3 \times \text{cm}^{-1}$ is an approximation of the zero-order energy of the $\pi-\pi^*$ state. ^d Obtained by adding the result of column two to E_{MLCT} . ^e Difference of zero-order ¹MLCT energy and observed ³MLCT energy. ^f With approximation of energy of first band in emission.

(bpy)₂(py)₂]²⁺. This material, when in solid form, appears blue-black due to the low energy of its charge-transfer transitions; no visible-region luminescence is detectable for this material. Again, as for [Ru(bpy)₂(en)]²⁺, the $d-\pi^*(\chi)$ transition occurs on the low-energy side of the $\pi-\pi^*$ transitions. The lowest energy bands in the absorption of this complex derive from excitation of the $d-\pi^*(\psi)$ state, and occur at approximately 520 nm ($19.2 \times 10^3 \text{ cm}^{-1}$). The intense $\pi-\pi^*$ transitions of this species occur at 287 nm ($34.8 \times 10^3 \text{ cm}^{-1}$), leading to an energy separation of these states on the order of $15.6 \times 10^3 \text{ cm}^{-1}$, much larger than observed in the complexes presented here. [For this reason, the energy of the $\pi-\pi^*$ transition in this complex is used as the zero-order energy of the $\pi-\pi^*$ state in the species that contain higher energy ¹MLCT states.]

The zero-order energy of the ¹MLCT bands in each of the high-energy complexes is more difficult to obtain but may be approximated with some degree of accuracy. These energies cannot be obtained from any other complexes, since other complexes have distinctly different MLCT energies owing to the different ligand field stabilizations of the metal. However, as mentioned previously, we may take the energy perturbation of the MLCT state as equal to that of the $\pi-\pi^*$ state using no more than second-order PT. Thus, the zero-order energy of the ¹MLCT transition should be given by the sum of the observed energy of the transition and the perturbation energy of the $\pi-\pi^*$ state as obtained by subtracting $34.8 \times 10^3 \text{ cm}^{-1}$ from the observed energy of this latter transition, as shown below:

$$E_{\text{MLCT}}^0 = E_{\text{MLCT}} + (E_{\pi-\pi^*} - 34.8 \times 10^3 \text{ cm}^{-1}) \quad (2)$$

To evaluate whether the movement of the $\pi-\pi^*$ state originates from an interaction between this state and the ¹MLCT, a plot must be made with eq 1 of the deviation of the $\pi-\pi^*$ energy vs the gap between the zero-order energies of the respective states. Table II presents data for many of the complexes of this study and gives the parameters for the plot that is shown as Figure 8. The [Ru(i-biq)₃]²⁺ complex is omitted because the zero-order energy is unknown for that ligand-localized transition; also, there is no guarantee that the perturbation would be of the same magnitude as that of bpy species. [Ru(bpy)₂(en)]²⁺ is omitted because the state under investigation there is the $d-\pi^*(\chi)$.

The linearity ($R = 0.99$) and the near-zero intercept of this plot indicate that the variation in energy of the $\pi-\pi^*$ absorbance in these materials with high-energy charge-transfer states is due in large part to a perturbation arising from the ¹MLCT. What is revealed here that is not evident with a cursory evaluation is that a similar perturbation of the ¹MLCT state is occurring.

We note that this phenomenon is not restricted to ruthenium-chelate complexes. Previous work by others in this laboratory⁷ determined that the $\pi-\pi^*$ transition of bipyridine is also perturbed significantly to higher energy in [Rh(bpy)₃]³⁺ and [Ir(bpy)₃]³⁺.

This raises the issue of skewing of the ¹MLCT bands in these complexes toward higher energy. Previous studies¹² have indicated without proof that this effect, which is seen in some phosphine-containing complexes, arises from an increase in charge-transfer

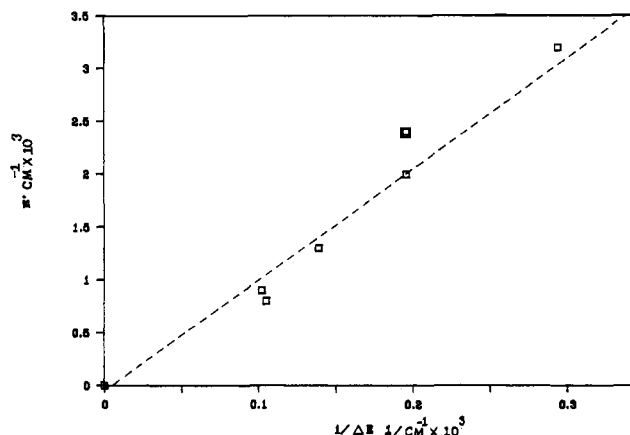


Figure 8. $E(\text{perturbation})$ vs energy separation, the variation of the energy of perturbation of the ¹ $\pi-\pi^*$ state as a function of the approximate separation of the zero-order ¹ $\pi-\pi^*$ and ¹MLCT states (see text for description of the procedure by which these parameters were calculated). Parameters: $y = a + bx$, $r = 0.9875$, $a = -0.11$, $b = 10.93$.

(i.e., charge-separation) character when the state occurs at high energy. The justification for this argument is that as the metal- and ligand-localized orbitals are further apart in energy, less mixing occurs between the d and π^* orbitals. However, the present work indicates that an opposing force is at work reducing CT character in the ¹MLCT transition—the mixing of the ¹MLCT and ¹ $\pi-\pi^*$ states.

The change in the absorption profile seen for these complexes is indeed correlated with the energy of the transition. This change in band shape may be analyzed with first-order PT, treating vibronic transitions occurring at higher energy than the 0-0 absorbance as separate entities capable of coupling independently to the $\pi-\pi^*$ state

$$\psi' = \frac{\langle \psi_{\pi-\pi^*}^0 | \hat{O} | \psi_{\text{MLCT}}^0 \rangle}{E_{\pi-\pi^*}^0 - E_{\text{MLCT}}^0} \psi_{\pi-\pi^*}^0 \quad (3)$$

where \hat{O} is an operator that couples the states.

Equation 3 gives the PT formula for first-order wave function correction. To calculate the intensity of a transition between the ground state and the excited Ψ_{MLCT} state, the square of the transition moment must be calculated as in

$$I = M^2 = [\langle \psi_{\text{MLCT}}^0 | \hat{r} | \psi_g \rangle + k \langle \psi_{\pi-\pi^*}^0 | \hat{r} | \psi_g \rangle]^2 \quad (4)$$

This equation illustrates that the intensity observed derives from both the zero-order MLCT wave function and the first-order perturbation term. If we take the energy separation of the zero-order $\pi-\pi^*$ state and Ψ_{MLCT} , as $E_{\pi-\pi^*}^0 - E_{\text{MLCT}}^0 - E_v$, where E_v is the vibrational energy that separates the states $\Psi_{\text{MLCT},v}$ from the 0-0 origin of the ¹MLCT transition, eq 4 may be rewritten

$$I = \left(C_1 + C_2 \frac{1}{1 - \frac{E_v}{\Delta E^0}} \right)^2 \quad (5)$$

where $C_1 = \langle \psi_{\text{MLCT}}^0 | \hat{O} | \psi_g^0 \rangle$, $C_2 = [\langle \psi_{\pi-\pi^*}^0 | \hat{O} | \psi_{\text{MLCT},v}^0 \rangle \langle \psi_{\pi-\pi^*}^0 | -\hat{O} | \psi_g^0 \rangle] / \Delta E^0$, and $\Delta E^0 = E_{\pi-\pi^*}^0 - E_{\text{MLCT}}^0$. So long as the vibronic levels we are examining are close in energy to the ${}^1\text{MLCT}$ origin, we may take $E_v/\Delta E^0$ to be small and replace $(1 - E_v/\Delta E^0)^{-1}$ with its approximation, $1 + E_v/\Delta E^0$. Dropping the second-order term in $E_v/\Delta E^0$ gives eq 6. This expression then includes terms that

$$I \approx C_1^2 + 2C_1C_2 \left(1 + \frac{E_v}{\Delta E^0} \right) + C_2^2 \left(1 + 2\frac{E_v}{\Delta E^0} \right) \quad (6)$$

are linear with respect to E_v , the energy separation of the vibronic level of the ${}^1\text{MLCT}$ absorbance from the origin. Thus, if the ${}^1\text{MLCT}$ transition had no oscillator strength of its own, it could obtain intensity by coupling with the $\pi-\pi^*$ transition and then the intensity would be skewed to higher energy. Evidence for this is presented in the discussion below.

In qualitative terms, the previous analysis indicates that the vibronic satellites of the ${}^1\text{MLCT}$ transition will be increasingly perturbed as their zero-order energies approach the $\pi-\pi^*$ transition. A question that remains to be addressed is what is the nature of the perturbation operator that produces the interaction between the $\pi-\pi^*$ state and the ${}^1\text{MLCT}$ state. The possibility of SOC interactions between these two singlet states would appear to be minimal at best; evidence from triplet state measurements indicates that this interaction is small, and so, the ${}^1\pi-\pi^*$ and ${}^1\text{MLCT}$ states should have no spin angular momentum to a good approximation.

A geometric perturbation or configuration interaction could also be responsible for the observed interaction, the former depending upon distortion to reduce symmetry, the latter depending upon the repulsion of electrons.

Much work has been done by Lim,¹³ investigating the vibronic interaction of $\pi-\pi^*$ states and $n-\pi^*$ states of azaromatic organic compounds. In many respects, the $d-\pi^*$ state of importance here resembles the $n-\pi^*$ state, but the t_{2g} orbital set is nominally nonbonding in character. The energy of interaction for such a mechanism is related to the displacement of the potential energy surface from the equilibrium position, giving rise to small perturbations of the zero-point energy of the lower state involved in two-state coupling until multiple minima occur (in a strong-coupling limit). If the splitting observed is due to this mechanism, the ${}^1\pi-\pi^*$ and ${}^1\text{MLCT}$ states would have to be displaced relative to one another along the vibrationally active mode. Since previous work^{1,10} has shown that the ${}^1\pi-\pi^*$ and ${}^1\text{MLCT}$ transitions are two states that have different electronic symmetries, this vibrationally active mode would have to be non-totally symmetric; either the ${}^1\text{MLCT}$ or the ${}^1\pi-\pi^*$ states would have to be distorted in such a manner as to remove some symmetry elements of the monomeric chromophore. This is, in effect, a specific form of geometric perturbation.

Emitting States. Since an interaction exists between the *singlet* ligand-localized and charge-transfer transitions, some interaction may also be expected to occur in the triplet emitting states. The magnitude of the interaction need not be the same as for the previous case, since the relative positions of the zero-point energies of the two triplet states in the multidimensional normal-coordinate space may not be the same.

What is apparent, however, is that in these complexes the ${}^3\text{MLCT}$ and ${}^1\text{MLCT}$ states do not derive from the same orbital configuration. This conclusion derived from the large variation in Stokes shifts for these molecules. For $[\text{Ru}(\text{bpy})_3]^{2+}$, the Stokes shift between the MLCT absorbance and emission is approximately $4.5 \times 10^3 \text{ cm}^{-1}$ (absorbance at 460 nm and emission at 578 nm), and this is near the range seen for most other Ru(II) complexes when their ligand field splitting is not of lower symmetry than D_3 . However, in the present complexes, the Stokes shift varies from a low of $6.0 \times 10^3 \text{ cm}^{-1}$ for $[\text{Ru}(\text{bpy})_2(\text{CNMe})(\text{CN})]^{1+}$ to a high of $8.6 \times 10^3 \text{ cm}^{-1}$ for $[\text{Ru}(\text{bpy})(\text{dppe})_2]^{2+}$. This conclusion,

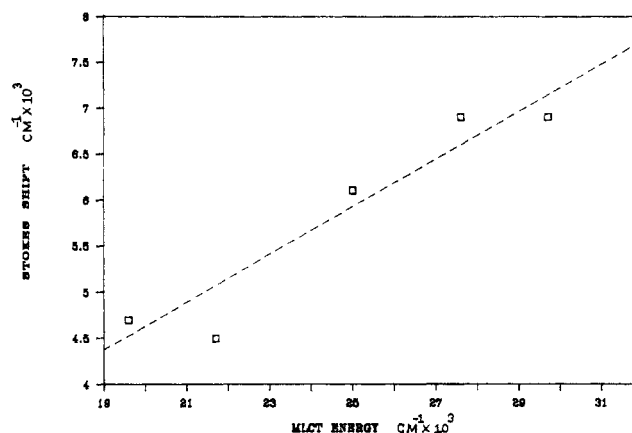


Figure 9. Stokes shift vs $E(\text{MLCT})$, the variation of the Stokes shift (defined by the energy separation between the zero-order ${}^1\text{MLCT}$ absorbance and ${}^3\text{MLCT}$ emissions) as a function of the energy of the absorbing ${}^1\text{MLCT}$ state. Parameters: $y = a + bx$, $r = 0.966$, $a = -0.61$, $b = 0.259$.

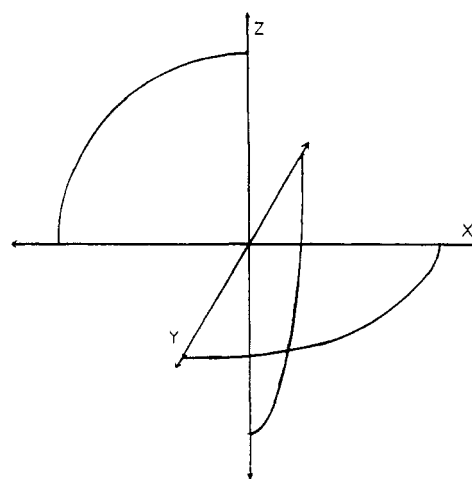


Figure 10. Orgel axes, the axis notation used by Orgel⁸ for calculations upon the metal basis functions of diimine chelate complexes.

that different orbital configurations are responsible for the ${}^1\text{MLCT}$ absorbing and ${}^3\text{MLCT}$ emitting states, is supported by the analysis of the polarization properties of the states.

Figure 9 shows the variation of the Stokes shift with the energy of the ${}^1\text{MLCT}$ transition. The latter energy is used as a measure of the impact that the odd ligands have on the t_{2g} orbital set of the metal. In this case, examination of the characteristics of complexes that contain two bipyridines and an odd regime, either a single symmetric bidentate ligand or two identical monodentate ligands *cis* to one another, can be done. This procedure yields a plot that is relatively linear, though scatter in the points is unavoidable due to the low number of significant figures available. However, data from complexes not conforming to the constraints given above (e.g., $[\text{Ru}(\text{bpy})(\text{dppe})_2]^{2+}$) are not on the line defined by the complexes with two bipyridines and symmetric bidentate/monodentate ligands.

The basis of the linear relationship revealed here is that, among the symmetry-adapted metal orbitals that may combine with the odd-ligand π -symmetry antibonding orbitals resulting in larger ligand field splitting, only one will be of the proper symmetry to do so.¹³ When the symmetry-adapted metal orbitals are obtained for the bipyridine units as linear combinations of the system utilized for the odd ligand, we find that, in addition to splitting produced by the bipyridine species, splittings between the metal orbitals are linear with respect to the magnitude of π back-bonding between the odd-ligand and the metal orbitals. The magnitude of the Stokes shift should be dependent upon this splitting of the metal orbitals involved in the ${}^1\text{MLCT}$ and ${}^3\text{MLCT}$ states if these are of different orbital origins. Hence, a linear relationship results

(13) (a) Lim, E.; Yu, J. *J. Chem. Phys.* **1968**, *49*, 3878. (b) Lim, E. In *Excited States*; Lim, E., Ed.; Academic: New York, 1979; Vol. 3, p 305. (c) Lim, E.; Yu, J. *J. Chem. Phys.* **1967**, *47*, 3270.

TABLE III: Symmetry-Adapted Linear Combinations of Metal t_{2g} Orbitals, Having Appropriate Symmetries in Each Monomer Axis System of a Tris Complex

Ru-ligand unit	normalized sym	SALC
1	b_1	$1/2(d_{xz} - d_{yz})$
1	a_1	d_{xy}
1	a_2	$1/2(d_{xz} + d_{yz})$
2	b_1	$1/2(d_{xy} - d_{yz})$
2	a_1	d_{yz}
2	a_2	$1/2(d_{xy} + d_{yz})$
3	b_1	$1/2(d_{xy} - d_{xz})$
3	a_1	d_{xz}
3	a_2	$1/2(d_{xy} + d_{xz})$

from plotting the Stokes shift versus the zero-order energy of the 1 MLCT state (which also depends upon the magnitude of odd-ligand π back-bonding).

To evaluate this in a more quantitative fashion, we adopt the axis designations of Orgel⁸ as shown in Figure 10; the alternative system described by Kober and Meyer¹⁴ is more cumbersome for this purpose. We wish to develop the symmetry-adapted linear combinations (SALC) of the t_{2g} orbital set that transform as a_1 , a_2 , and b_1 in each of the C_{2v} units of the complete molecule as an aid to understanding the effect that the odd ligand will have on the MLCT states of the Ru-bpy chromophore. Table III lists these functions, based upon the Orgel system of Figure 10.

We now assume that the π acceptor orbitals of the odd chelate, either a single bidentate or two monodentate ligands, have b_1 orbital symmetry as does bipyridine. This is not an unreasonable assumption since this acceptor orbital should result from the least antibonding combination of π -symmetry orbitals of the two acceptor atoms. Therefore, only a single SALC wave function has the appropriate symmetry to combine with the acceptor wave function, i.e., the b_1 . This would then be the linear combination that would be stabilized in energy by π back-bonding with the odd chelate.

To determine the effect that this back-bonding would have upon the energies of the different MLCT states, we may simply determine the extent to which the b_1 SALC wave functions of the odd ligand overlap with those of the bipyridine states; those with the greatest overlap would be stabilized the most. Any metal function of the Ru-bipyridine unit that did not have any overlap with the stabilized SALC of the Ru-odd-ligand unit would be unaffected by the back-bonding occurring between the metal and that ligand.

The SALC orbitals of the relevant Ru-bpy unit may be written in terms of the SALC orbitals of the odd-ligand unit, and thus, the mixing coefficients demonstrate that the effect of ligand field splitting by the strong-field ligand upon the a_1 , a_2 , and b_1 metal orbitals of the Ru-bpy unit is to stabilize the b_1 and a_2 orbitals with half the magnitude of the a_1 . Therefore, when ligand field splitting of the metal is large enough, the a_1 metal orbital becomes lowest in energy, causing the emitting state to have orbital symmetry of either B_2 or A_1 . When ligand field splitting by the odd ligand is significantly less than that of bipyridine, we would find that the a_1 orbital is stabilized less than the other SALCs of the Ru-bpy unit, leading to an emitting state that is of B_1 total symmetry.

This is the trend that was evident in studies presented earlier: molecules with low-energy charge-transfer states, indicative of small ligand field splitting of the metal, produced photoselection results that could be modeled as an exchange of lowest orbital emitting states, exchanging the B_2 orbital state for the B_1 . However, the present results indicate that the separation between the a_2 and b_1 metal orbitals should be relatively unaffected by the magnitude of interaction with an odd ligand, and thus, it may be impossible to observe an emitting state with total orbital symmetry of A_1 (this would be easily identifiable by the negative polarization (P) value that this state should produce in photoselection studies).

With this information, the slope that is obtained in Figure 9 may be analyzed in terms of the additional splitting of the d orbitals by the strong-field odd ligand. To perform this analysis, we assume that the energy of the singlet state is given simply as the difference between the energies of the π^* orbital and the d orbital involved in the transition. For the energy of the triplet emitting state, the same approximation is used plus an added term describing the electron exchange stabilization of the triplet state, which we assume constant. These relationships are shown in eq 7, where E_s is the energy of the singlet transition, E_t is the energy

$$E_s \approx E_{\pi^*} - E_{d_1} \quad (7a)$$

$$E_t \approx E_{\pi^*} - E_{d_2} - E_{xchg} \quad (7b)$$

of the triplet transition, E_{π^*} and E_{d_1} are the energies of π^* and d orbitals, respectively, and E_{xchg} is the exchange stabilization of the triplet state. The measured Stokes shift then is simply the difference of these two energies. Obviously, when $d_1 = d_2$, the energy gap between the singlet and triplet should be only E_{xchg} and should be almost invariant.

We then calculate the differential of the Stokes shift energy with respect to the ligand field stabilization (represented by ηA) of the SALC of the odd ligand, as well as the differential E_s with respect to the same quantity. Dividing the former by the latter, a crude approximation of the slope expected in Figure 8 is obtained as a function of the d orbitals partially occupied in the singlet and triplet states, without the contrivance of a differential of the parameter η . This result is shown in eq 8.

$$\frac{dSS}{dE_s} = 1 - \frac{dE_{d_2}}{dE_{d_1}} \quad (8)$$

Since intensity mechanisms for the localized singlet absorbance and experimentally determined polarizations for absorbance have demonstrated that the absorbance is z-polarized, the transition must involve the b_1 orbital localized on the metal. The polarization of the luminescence has clearly demonstrated that the emission must not come from this same orbital configuration. Thus, the remaining permutations of orbitals involved in these two transitions are (b_1, a_2) and (b_1, a_1) , where the first symmetry is that of the orbital involved in the absorbance and the second is the orbital involved in the luminescence. For the former possibility, the calculated slope should be 0, since the crude modeling used here shows that these orbitals should remain stationary with respect to one another. For the latter instance, the calculated slope should be -1, since the a_1 orbital should be pushed to higher energy faster than the b_1 , causing the Stokes shift to narrow as ligand field interaction of the odd ligand increases.

The experimental value of the slope is 0.259, and thus, this crude treatment appears to be more consistent with the a_2 orbital being only partially occupied in the triplet state. This would give rise to an orbital state of B_2 symmetry, consistent with the conclusions obtained from polarization results¹⁵ for $[\text{Ru}(\text{bpy})(\text{CN})_4]^{2-}$ and those conclusions based upon modeling of the SSEXP for a series of mono, bis, and tris chelate complexes.¹⁰

Obviously, the calculated slope here is not precisely zero; however, the assumptions of the analysis could be responsible for this. It appears unlikely that the energy of interaction of the odd ligand should be exactly equal for the two orbitals concerned. Also, reduced interactions between the coordinated bipyridine and the metal orbitals due to the increased energy separation are not considered. Alterations in the exchange interactions that stabilize the triplet state are also not considered, nor are energy effects from spin-orbit coupling. The σ -donor effects are neglected, and changes in bond lengths are omitted. Also, it is assumed that the energies of states are given primarily by the differences in the energies of the orbitals undergoing the transition, and the assumption that the SALCs of the Ru-bpy unit are identical with

(14) Kober, E.; Meyer, T. *Inorg. Chem.* **1984**, *23*, 3877.

(15) Myrick, M. L.; Pittman, R. *J. Phys. Chem.*, to be submitted for publication.

the actual metal orbitals is implicit. Finally, though correction was made for the $^1\text{MLCT}$ interaction with the $^1\pi-\pi^*$, no correction was possible for the $^3\text{MLCT}$.

Apart from the analysis of the Stokes shift, quantitative information from the emitting state alone is more difficult to obtain than was the case for the absorbing state. For $[\text{Rh}(\text{bpy})_3]^{3+}$, the ligand-based phosphorescence that this complex produces has an apparent origin at 450 nm ($22.2 \times 10^3 \text{ cm}^{-1}$). A similar type of emission is found for $[\text{Ir}(\text{bpy})_3]^{3+}$ and $[\text{Ru}(\text{bpy})(\text{CNMe})_4]^{2+}$,⁸ and we may assume that this energy corresponds to the energy of the $^3\pi-\pi^*$ state in the absence of any perturbing effects from the $^3\text{MLCT}$.

Examination of the emission for the complexes presented leads to the observation that the relative magnitudes of the vibronic components of the emitting state are altered as the emitting state is moved to higher energy; this alteration has the effect of reducing the magnitude of the 0-0 transition and increasing that of its vibronic satellites relative to one another.

Unfortunately, a plot of the form of Figure 8 cannot be produced for the emission since the actual position of the $^3\pi-\pi^*$ state cannot be known. Since the emission spectra are uncorrected for detector response, quantitative comparisons of the magnitudes of individual bands in the emission spectra cannot be done. Moreover, the procedure that Lim¹² uses to analyze phosphorescence spectra of molecules undergoing vibronic perturbations is not possible due to the diffuse nature of the emission spectrum.

However, a qualitative comparison of the trend in the intensity components of the emission with that seen for the band contour $^1\text{MLCT}$ absorbance is feasible. The principal similarity between the two transitions appears to be that both seem to involve distorted excited states that have their intensity distributions affected by a perturbation with a higher lying state. However, the magnitude of the interaction between triplet states seems significantly smaller since alterations in the emission band shape are not noticeable until the states approach one another within approximately $3 \times 10^3 \text{ cm}^{-1}$.

Photoselection. Another unusual feature of the spectroscopy of these complexes is the SSEXP data obtained for them. As a particularly striking example, we take the photoselection of $[\text{Ru}(\text{bpy})(\text{dppe})_2]^{2+}$, a complex that is expected to possess a monomeric Ru-bpy chromophore and thus give large, featureless polarizations across the $^1\text{MLCT}$. Instead, the values measured are low and rise almost monotonically across the absorption band, attaining a maximum of only 0.19. This change in polarization characteristics is directly related to the mixing of the $^1\pi-\pi^*$ and $^1\text{MLCT}$ wave functions. To reduce P at high energy, some absorbance must be occurring that is polarized perpendicular to the metal-ligand axis. The states responsible for this absorbance may be vibronic states of the main absorbing $^1\text{MLCT}$ or may be associated with $^1\text{MLCT}$ states that have low absorption strength of their own. Two such singlet states exist, involving the a_1 or a_2 metal orbitals.

In several of the complexes presented here, such as $[\text{Ru}(\text{bpy})(\text{dppe})_2]^{2+}$, $[\text{Ru}(\text{bpy})_2(\text{dppe})]^{2+}$, and $[\text{Ru}(\text{i-biq})_3]^{2+}$, a weak shoulder appears on the low-energy edge of the $^1\text{MLCT}$ absorbance and is associated with reduced polarization in that region. It seems conceivable that this may represent the electronic origin of a second MLCT state, which borrows intensity from the $^1\pi-\pi^*$ transition.

In earlier work,¹⁰ it was pointed out that the large polarizations produced by monomeric complexes were due both to the absorbing state being linearly polarized and the emitting state having the same polarization. Since some interaction between the $^3\text{MLCT}$ emitting state and the $^3\pi-\pi^*$ state seems apparent, it is likely that the photoselection values are reduced for these complexes, in part because the emission polarization is no longer purely a linear-linear process as for the simple monomer. However, the structure seen for the photoselection spectrum across the $^1\text{MLCT}$ must be largely due to the interaction of that complex manifold of states with the nearby ligand-centered state.

The exact behavior of the SSEXP in these complexes is difficult to model due to the number of states involved; however, note that

the typical structure of the photoselection of cis and tris complexes is absent from these spectra. Indeed, the SSEXP of $[\text{Ru}(\text{bpy})_2(\text{dppe})]^{2+}$ is very similar to its monomeric analogue despite the knowledge that bis chelates¹ exhibit structure in their excitation polarization ratios due to the presence of localized and delocalized regions for the singlet absorption.¹⁰ This may indicate that the states are distorted to such an extent by interactions with the $^1\pi-\pi^*$ that localized portions of the excited singlet manifold do not exist.

$[\text{Ru}(\text{bpy})_2(\text{en})]^{2+}$ and $[\text{Ru}(\text{i-biq})_3]^{2+}$. These two complexes are dealt with separately due to their distinct spectral features. In particular, $[\text{Ru}(\text{bpy})_2(\text{en})]^{2+}$ is included among complexes with high-energy charge-transfer states because this complex affords an opportunity to examine a high-energy charge-transfer transition involving the χ -symmetry π^* orbital of bpy. The maximum of this transition occurs at 353 nm ($28.3 \times 10^3 \text{ cm}^{-1}$), comparable to the most strongly blue-shifted transitions involving the ψ orbitals of bpy, those of $[\text{Ru}(\text{bpy})_2(\text{CNH})_2]^{2+}$ and $[\text{Ru}(\text{bpy})_2(\text{CNMe})(\text{CNH})]^{2+}$. Little mention of this transition to $\chi(\pi)$ is made in the literature other than the fact that such a transition exists. However, the present investigations make apparent that the skewed appearance of this transition in the complex with ethylenediamine may not be due, in fact, to any great difference between the character of this and the lower energy MLCT. This band is similar in appearance to that of the $d-\pi^*(\psi)$ transitions that occur in this region, and photoselection results for this absorbance indicate that it may in fact be quite similar to the latter. A very enlightening comparison may be made between this absorbance and the $d-\pi^*(\psi)$ absorbance of $[\text{Ru}(\text{bpy})_2(\text{CNH})_2]^{2+}$. Each have maximum absorbance at nearly identical energies. The maxima they exhibit in the SSEXP spectra occur within 400 cm^{-1} of one another, and the values of those maxima are identical. In this case, however, the metal orbital that is of the proper symmetry to combine with the higher π^* of bpy is not the b_1 but the a_2 .¹⁴ Thus, the increase in the Stokes shift with increasing energy for the lower MLCT state should not be reflected in the upper transition, since this absorbance and the luminescence derive from the same orbital configuration of the metal.

$[\text{Ru}(\text{i-biq})_3]^{2+}$ is also not discussed with the other complexes, since it has two distinct features: First, the ligand is different so there is no way of clearly knowing when its ligand-based transitions are being perturbed without some unperturbed system to examine. Second, the complex exhibits a $\pi-\pi^*$ luminescence.⁹ Interestingly, however, this molecule also follows some trends evident in the bipyridine species. We note that photoselection across the $^1\text{MLCT}$ band of this complex is actually slightly negative. This would likely be the end result of the continuation of the high-energy shift in the bipyridine species, as the photoselection values decrease as energies of absorbance and emission move to higher energy. Also, the $^1\text{MLCT}$ transition is skewed to high energy, consistent with observations of the bpy complexes, and appears to possess some low-lying shoulders. Both of these phenomena, by analogy with the bpy species, are likely due to the coupling of the $^1\pi-\pi^*$ and $^1\text{MLCT}$ transitions.

Conclusions

The study of molecules that possess high-energy charge-transfer states has demonstrated an interaction between the $\pi-\pi^*$ and $^1\text{MLCT}$ states, likely of a vibronic origin. A perturbation theory treatment of interactions between states produced a plot with data for numerous complexes with a wide variation in state energies. These data indicate a correlation between the shift of the $^1\pi-\pi^*$ state and the zero-order energy separation of this state from the $^1\text{MLCT}$.

In addition, the luminescence of this series of complexes was studied. A correlation was noted between the Stokes shift (the energy separation between the lowest absorbance and the emission) and the zero-order energy of the $^1\text{MLCT}$ transitions of several complexes. These complexes had in common that they were all bis-chelates of bipyridine with an odd ligand, either a single symmetric bidentate ligand or two identical monodentate ligands in a cis configuration. For molecules that did not fit these limits, significant deviations from the near-linear relationship were seen.

These results indicate that singlet absorption and triplet emission derive from states of different orbital configurations, since the Stokes shift varied by a large amount over the complexes investigated. A crude modeling of the variation of Stokes shift with the magnitude of ligand-field stabilization of the odd ligand was done and indicated that the absorbance was into a state of A_1 total symmetry, and luminescence for most complexes arises from a triplet state that has an orbital symmetry of B_2 . This compared well with results obtained by other independent means.

The variation of the energies of the different orbital MLCT states was seen also to correspond to that determined with the ICC model.¹⁰ With strong-field π -back-bonding ligands, one of the metal orbitals of the t_{2g} set was stabilized more than the remaining two, whose energy separation was relatively unaffected. This led to an emitting state that would be of B_2 orbital symmetry consistent with the discussion above. However, replacement of

this odd ligand by one that is only a weak π -back-bonder would destabilize the metal orbitals to a lesser degree. Ultimately, this would lead to an emitting state of B_1 orbital symmetry. This appears to explain the results obtained and modeled for $[\text{Ru}(\text{bpy})_2(\text{en})]^{2+}$ and $[\text{Ru}(\text{bpy})_2(\text{NH}_3)_2]^{2+}$.¹⁰

Acknowledgment. This work was supported by a grant from the Army Research Office (Grant DAAL 3-86-1C-0400). M. L.M. was supported by a National Science Foundation Graduate Fellowship.

Registry No. $[\text{Ru}(\text{bpy})_2(\text{dppe})](\text{PF}_6)_2$, 119679-84-4; $[\text{Ru}(\text{bpy})_2(\text{dppe})_2](\text{PF}_6)_2$, 122382-97-2; $[\text{Ru}(\text{bpy})_2(\text{dmpe})](\text{PF}_6)_2$, 122408-26-8; $[\text{Ru}(\text{bpy})_2(\text{CNMe})(\text{CN})]^+$, 116699-20-8; $[\text{Ru}(\text{bpy})_2(\text{CNMe}_2)_2]^{2+}$, 116670-12-3; $[\text{Ru}(\text{i-biq})_3](\text{PF}_6)_2$, 75778-38-0; $[\text{Ru}(\text{bpy})_2(\text{en})](\text{ClO}_4)_2$, 31659-06-0; $[\text{Ru}(\text{bpy})_2(\text{CNH})_2]^{2+}$, 72147-15-0; $[\text{Ru}(\text{bpy})_2(\text{CNMe})(\text{CNH})]^{2+}$, 122382-98-3; $[\text{Ru}(\text{bpy})_3]^{2+}$, 15158-62-0.

Effects of the Transition Dipole in Raman Scattering

Song Ling, Dan G. Imre, and Eric J. Heller*

Department of Chemistry BG-10, University of Washington, Seattle, Washington 98195
(Received: March 17, 1989)

We use the time-dependent theory of Raman scattering to investigate, both semiclassically and quantum mechanically, the effects of nonconstant transition dipoles on Raman excitation profiles and total Raman emission spectra. The system with a single excited electronic state dominating the scattering process is studied. Semiclassical analytic formulas are derived that can be used to obtain information of the transition dipole and the excited-state surface. Depending on the parameters, significant deviations from the previous works on the Raman scattering, where the constant transition dipole (Condon approximation) was invoked, are observed.

I. Introduction

The time-dependent theory of Raman scattering has been developed¹ as a physically equivalent, but computationally much more feasible alternative to the usual energy frame Kramers-Heisenberg-Dirac (KHD) formulation.³ Using the time-dependent formulation of Raman scattering as a springboard, short-time semiclassical dynamics has been used to derive formulas and rules governing certain aspects of Raman spectroscopy.² We call these the "simple aspects of Raman spectroscopy". These rules depend on the validity of certain simplifying assumptions, principally: (1) transition dipole moments independent of the nuclear coordinates (the Condon approximation); (2) dominance of one Born-Oppenheimer potential energy surface over others (e.g., being in or near resonance with an isolated potential energy surface with a reasonably large transition dipole to the ground Born-Oppenheimer surface), and (3) short-time semiclassical approximation to the dynamics, based on Taylor expansion of the local potential energy surface.

The time-dependent formulation of Raman scattering allows prediction and interpretation of Raman spectra in a variety of otherwise complex situations, such as polyatomic molecular resonance Raman spectra and Raman spectra of dissociating molecules. The "simple aspects" formulas go one step further in simplicity (i.e., with the above three further approximations that are not intrinsic to the time-dependent formalism). Morris and Woodruff⁴ also improved and extended the "simple aspects"

formulas, to include the simultaneous effects of first and second derivatives in the local potential energy surface in the Franck-Condon region. However, the Condon approximation was not relaxed in their work.

Experimental spectra sometimes show strong deviation from the simple rules based on the Condon approximation.⁵ The question of the possible role of the transition dipole in producing these deviations naturally arises. In the past few years much work on Raman scattering has taken into consideration the non-Condon effects. Among them are Champion, Albrecht, Stallard, and Callis's work,⁶ where the KHD formula serves as a starting point, and Tehver,⁷ Chan,⁸ Tonks, Lu, and Page's work,⁹ where a time-dependent formalism was adopted. These full quantum mechanical treatments are exact in principle and have other advantages like including the finite temperature effects into computation. Also the "transform" techniques developed by the above workers have shown usefulness in extracting information from experimental Raman spectra.

In this paper, our main purpose is to remove the biggest offender in the "simple aspects" assumptions, namely, the Condon approximation, within the framework of the wave packet evolution approach. This method has some features distinctive from other treatments mentioned above; e.g., the overlaps between the moving wave packet in the excited potential surface, times the transition dipole function and the eigenfunctions of the ground potential surface, again times the dipole, form the kernel functions in the

(1) Lee, S.-Y.; Heller, E. J. *J. Chem. Phys.* **1979**, *71*, 4777. Tannor, D. J.; Heller, E. J. *J. Chem. Phys.* **1982**, *77*, 202. Myers, A. B.; Methies, R. A.; Tannor, D. J.; Heller, E. J. *J. Chem. Phys.* **1982**, *77*, 3857. Heller, E. J. *Acc. Chem. Res.* **1981**, *14*, 368.

(2) Heller, E. J.; Sundberg, R. L.; Tannor, D. *J. Phys. Chem.* **1982**, *86*, 1822.

(3) See, for example: Louisell, W. H. *Quantum Statistical Properties of Radiation*; Wiley: New York, 1973.

(4) Morris, D. E.; Woodruff, W. H. *J. Phys. Chem.* **1985**, *89*, 5795.

(5) Zhang, J.; Imre, D. G. *J. Chem. Phys.* **1989**, *90*, 1666.

(6) Champion, P. M.; Albrecht, A. C. *Annu. Rev. Phys. Chem.* **1982**, *33*, 353. Stallard, B. R.; Champion, P. M.; Callis, P. R.; Albrecht, A. C. *J. Chem. Phys.* **1983**, *78*, 712.

(7) Tehver, I. *J. Opt. Commun.* **1981**, *38*, 279.

(8) Chan, C. K. *J. Chem. Phys.* **1984**, *81*, 1614.

(9) Tonks, D. L.; Page, J. B. *Chem. Phys. Lett.* **1981**, *79*, 247. Tonks, D. L.; Page, J. B. *J. Chem. Phys.* **1988**, *88*, 738. Lu, H. M.; Page, J. B. *Chem. Phys. Lett.* **1986**, *131*, 87. Lu, H. M.; Page, J. B. *J. Chem. Phys.* **1988**, *88*, 3058.